Available online at www.sciencedirect.com
SCIENCE DIRECT
International Journal of Machine Tools & Manufacture 45 (2005) 1717–1725
INTERNATIONAL JOURNAL OF MACHINE TOOLS & MANUFACTURE DESIGN, RESEARCH AND APPLICATION
www.elsevier.com/locate/ijmactool

Investigation of wire electrical discharge machining of thin cross-sections and compliant mechanisms

Scott F. Miller[a], Chen-C. Kao[a], Albert J. Shih[a,*], Jun Qu[b]

[a]*Mechanical Engineering, University of Michigan, Ann Arbor, MI 48109, USA*
[b]*Oak Ridge National Laboratory, Metals and Ceramics Division, Oak Ridge, TN 37831, USA*

Received 30 September 2004; accepted 3 March 2005
Available online 12 April 2005

Abstract

The wire electrical discharge machining (EDM) of cross-section with minimum thickness and compliant mechanisms is studied. Effects of EDM process parameters, particularly the spark cycle time and spark on-time on thin cross-section cutting of Nd–Fe–B magnetic material, carbon bipolar plate, and titanium are investigated. An envelope of feasible wire EDM process parameters is generated for the commercially pure titanium. The application of such envelope to select suitable EDM process parameters for micro feature generation is demonstrated. Scanning electron microscopy (SEM) analysis of EDM surface, subsurface, and debris are presented. SEM observations lead to a hypothesis based on the thermal and electrostatic stress induced fracture to explain the limiting factor for wire EDM cutting of thin-sections. Applications of the thin cross-section EDM cutting for manufacture of compliant mechanisms are discussed.

Keywords: Wire EDM; Compliant mechanism; Material removal rate

1. Introduction

The development of micro mechanical components, the growing needs for micro-feature generation, and applications of advanced, difficult-to-machine materials have made the wire EDM an important manufacturing process to meet these demands. The wire EDM process uses electrical sparks between a thin, traveling wire electrode and the workpiece to erode the work-material and generate the desired shapes. The cutting force is low, which makes the EDM an important process to manufacture precise, intricate, and miniature features on mechanical components.

The information to select proper wire EDM process parameters for newly developed materials or micro features is not readily available [1]. Manufacturers of EDM machines usually provide a database of suggested process parameters for commonly used work- and electrode-materials under typical operating conditions. Such database cannot meet the growing new EDM applications, including the machining of miniature features. The goal of this study is to investigate the effect of two important wire EDM process parameters, spark cycle and spark on-time, on the thin-section cutting of sintered Nd–Fe–B magnet, titanium, and carbon–carbon bipolar plate.

The EDM machine converts the electrical energy into thermal energy in the plasma discharge channel during the spark discharge. The thermal energy melts and vaporizes workpiece material during the process. The molten work- and electrode-materials solidify on the work surface and create a recast layer [2]. The high temperature has two effects. First, a heat affected zone under the recast layer is created [2]. Second, the high temperature generates the thermal stress in the workpiece. As will be seen in this research, the thermal stress could affect the minimum thickness of the workpiece in wire EDM.

The micro EDM has been studied extensively by Masuzawa and his research group in the past two decades [3–5]. In addition, Luo [6] investigated the EDM with a small erosion area by examining effects of spark off time. Takahata and Gianchandani [7] studied the use of electrode arrays for batch EDM generation of micro-features. Furutani et al. [8,9] developed the dot-matrix EDM method using the thin wire electrode to produce various micro

* Corresponding author. Tel.: +1 734 647 1766; fax: +1 734 936 0363.
E-mail address: shiha@umich.edu (A.J. Shih).

0890-6955/$ - see front matter © 2005 Elsevier Ltd. All rights reserved.
doi:10.1016/j.ijmachtools.2005.03.003

shapes with the μm level accuracy. Rajurkar and Yu [10] expanded the micro EDM technology using CAD/CAM. Hori and Murata [11] studied the wire EDM of micro involute spur gears. Yu et al. [12] presented a theoretical model for micro EDM surface profile generation and incorporating the tool wear effect. More recently, Kaminski and Capuano [13] and Zhao et al. [14] studied the EDM micro hole machining.

An envelope of material removal rate (MRR) was defined and generated for a variety of advanced materials to aid the selection of process parameters for wire EDM [1,15]. Such envelope can be applied to setup the wire EDM process for fast, high MRR machining. A rough surface with a thick recast layer is usually generated in high MRR EDM. Another application of the wire EDM envelope, more relevant to this study, is the selection of process parameters for slow, low MRR EDM cutting to enable the machining of micro-features and generate surfaces with improved integrity. In this study, the envelope of feasible wire EDM process parameters for commercially pure titanium, denoted as Ti, is created. The envelope is employed to machine the Ti with thin cross-section. The Ti material is selected because of its biocompatibility for human implant applications.

This study explores the use of wire EDM for manufacturing of compliant mechanisms. Compliant mechanisms are defined as the jointless mechanisms where the elastic deformation is intended as a source of motion [16]. The thin-section is used to generate the deformation and motion of compliant mechanisms. Wire EDM is a process of choice for the fabrication of compliant mechanisms. Wire EDM of miniature titanium compliant mechanisms, which have the potential for medical applications, is investigated. The MRR process envelope of Ti is applied to select suitable EDM process parameters.

The experimental setup and procedure of the wire EDM machine are first discussed. Results of the Ti MRR envelope and thin cross-section cutting of various materials are then presented. The scanning electron microscope (SEM) is applied to analyze debris captured in wire EDM. The effect of thermal stress on thin-section wire EDM is investigated. Finally, applications of micro-feature generation, including the compliant mechanism, are discussed.

2. Experimental setup and work-materials

2.1. Wire EDM machine setup

The EDM experiments are conducted on a Brother HS-5100 wire EDM machine using the brass wire with 0.25 mm nominal diameter. Two EDM process parameters studied are the spark cycle, T, and spark-on time, T_{on}. Fig. 1 shows a typical waveform of voltage between the workpiece and wire electrode during EDM. The spark cycle, T, is the period of change in voltage. The spark on-time or pulse on-time, T_{on}, is the duration in a spark cycle that the voltage is built up. For the Brother HS-5100, the range of spark on-time (T_{on}) is from 2 to 18 μs and spark cycle, T, is from 10 to 1000 μs. The wire tension is 15 N, and the gap voltage between the wire and electrode was set at 35 V.

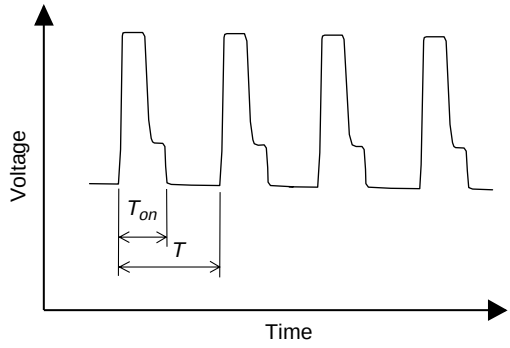

Fig. 1. Definition of the spark cycle, T, and spark on-time, T_{on}, in the EDM spark cycle.

2.2. Work-materials

Three work materials investigated in this study are the sintered Nd–Fe–B permanent magnet, grade two commercially pure Ti, and carbon–carbon bipolar plate. Properties of Nd–Fe–B magnet, which has high magnetic density and is used for miniature, energy-efficient electrical motor, actuator, and generator applications, and the carbon–carbon bipolar plate, which is used for proton exchange membrane fuel cell, have been discussed in the previous research [1,15].

2.3. Experimental setup and procedure

The 1.5 mm thick Nd–Fe–B plate, 2.3 mm thick carbon–carbon bipolar plate, and 1 mm thick Ti plate are used to investigate the effect of T and T_{on} on the thin-section EDM cutting. The envelope of feasible wire EDM process parameters for Nd–Fe–B and carbon–carbon bipolar plate have been presented in Ref. [1] and are applied for both high and low MRR EDM cutting. The high MRR EDM cutting requires high energy density, creates thick recast layers and surface damages, and limits the minimum thickness in thin-section cutting. On the contrary, the low MRR EDM is a slow process, but it is more suitable for machining thin-sections and micro-features.

The setup of thin-section EDM cutting experiment is shown in Fig. 2. The EDM cuts parallel grooves in a plate and leaves a thin section of thickness t. The same set of process parameter is repeated and the thickness cut is reduced each time until the minimum thickness of the thin-section is achieved.

Tests are conducted to find minimum thickness for a specific T_{on}. When the T_{on} is high, the electrical spark energy is strong, thermal shock due to thermal stress is

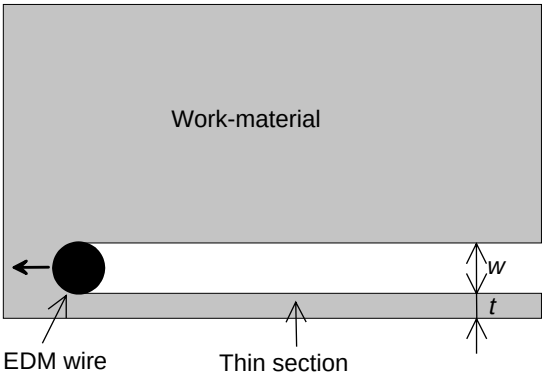

Fig. 2. Wire EDM experiment setup to cut thin section.

large, and wire feed rate or MRR is high. On the other extreme, when T_{on} is low, the electrical spark energy is weak, energy delivered during cutting is small, and wire feed rate or MRR is low. The MRR is usually high at higher T_{on}. The minimum thickness in wire EDM, as observed in this study, is more dependent on T_{on} than T.

The machine, material, and physical limitations such as debris flushing determine the minimum thickness in wire EDM thin section cutting. To determine the feasible envelope, sets of wire EDM tests are first conducted for specific pulse on-time, T_{on}, at 2, 6, 10, 14, and 18 μs. For the wire EDM machine used in this study, 2 and 18 μs are the lower and upper limits for T_{on}, respectively. Under the same T_{on}, the spark cycle, T, is varied. Without knowing the behavior of new work-materials processed by EDM, different levels of T have to be tested. To determine the minimum thickness of the thin section under certain spark energy, the binary-section method was applied. First, a relatively large thickness (t_0) for cutting was tried. Then the second thickness was set to be $t = t_0/2$. If this succeeded, tested thickness was $t = t_0/4$, otherwise $t = 3t_0/4$ was tested. The same step was repeated until the change in thickness value was close to 25 μm. The length of cut is at least 3 mm, about 12 times the diameter of the wire.

3. Wire EDM experimental results

3.1. Ti MRR envelope and thin-section cutting

The wire EDM MRR envelope of the feasible T and T_{on} for 1 mm thick Ti is generated. The Ti material and its MRR envelope are then applied for the thin-section cutting and later, in Section 6, for machining of compliant mechanisms.

The experimental procedure to find the envelope of feasible T under a specific T_{on} has been presented in [1]. For a set T_{on}, the machine limits of short circuit and wire breakage constrains the T and MRR. Limits imposed by the EDM machine used in this study, including the 2–18 μs T_{on} and the maximum slide speed, complete the boundaries of an envelope.

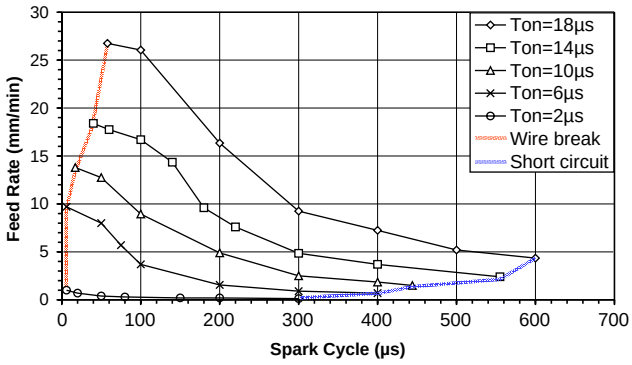

Fig. 3. Envelope of feasible wire EDM process parameters for Ti.

The wire EDM envelope for 1 mm thick Ti is shown in Fig. 3. The $T_{on} = 18$ and 2 μs are the top and bottom boundaries. The wire break and short circuit are the left and right boundaries, respectively. Compared to other envelopes presented in [1], the Ti has a broad selection of MRR at low spark cycle T. For example, at $T = 60$ μs, a wide range of feed rate, from almost the highest 27 mm/min to the lowest 0.5 mm/min, can be achieved. Two process conditions at two extreme sides of $T = 100$ μs, i.e. $T_{on} = 2$ and 18 μs, are used in the following thin-section EDM cutting tests.

Results of thin-section cutting of Ti with $T_{on} = 2$ and 18 μs are shown in Fig. 4(a) and (b), respectively. Fig. 4(a) illustrates the 61 μm thickness section machined using $T_{on} = 2$ μs and 0.5 mm/min wire feed rate. The MRR is small but thinner cross-section can be machined. When the T_{on} is increased to 18 μs, the wire feed rate is increased to 26 mm/min but the minimum thickness is increased to 165 μm. This illustrates the effect of EDM process parameter selection on micro-feature generation.

Another phenomenon observed in Fig. 4 is the bending of thin-section to the right. All grooves were cut from left to right. The bending is due to the thermal stress generated during the EDM process.

3.2. Carbon–carbon bipolar plate and Nd–Fe–B magnet thin-section cutting

For the carbon–carbon bipolar plate, two sets of process parameter with the highest MRR ($T_{on} = 18$ μs and $T = 60$ μs) and lowest MRR ($T_{on} = 4$ μs and $T = 1000$ μs) are experimented. The minimum thickness of the section cut by the wire EDM, as shown in Fig. 5(a), is 2.7 mm for the high MRR and 1.2 mm for the low MRR EDM cutting.

Another set of thin section wire EDM tests was conducted on the sintered Nd–Fe–B magnet. Results are shown in Fig. 5(b). Under $T_{on} = 2$, 10, and 18 μs with respective $T = 80$, 120, and 150 μs, the minimum thickness is 0.20, 0.75, and 1.15 mm, respectively, for the Nd–Fe–B magnet. The flushing of de-ionized water was applied during the EDM process.

The effect of water flushing on the minimum thickness was also experimented. Table 1 compares results from EDM

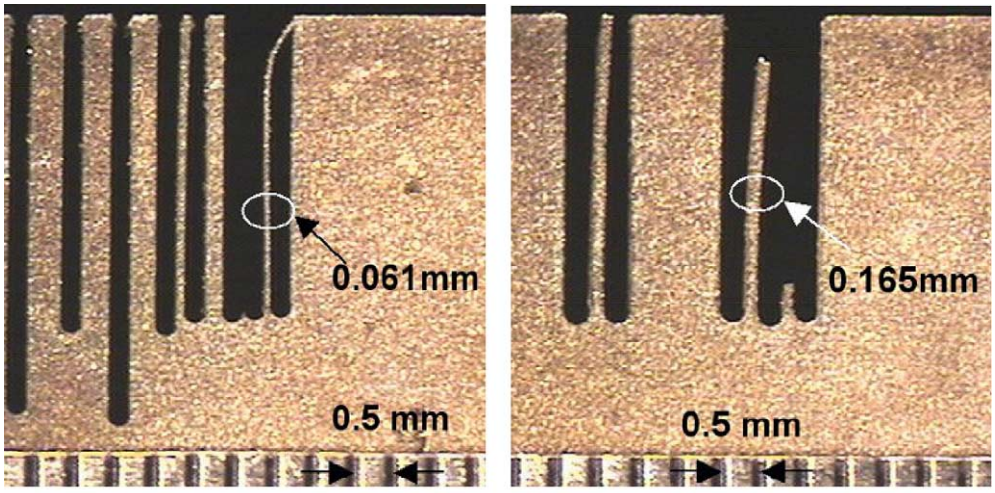

Fig. 4. Results of thin-section wire EDM of Ti with $T=100$ μs: (a) $T_{on}=2$ μs and (b) $T_{on}=18$ μs. Noted the grooves cut from left to right and the bending created by thermal stress.

thin-section tests with and without water flushing. It is noted that flushing will clean the debris from the gap between wire electrode and workpiece and can improve the MRR. However, flushing generates a force on the workpiece. This force can be detrimental for the thin-section or micro-feature machining due to the bending and possibly fracturing of the miniature workpiece during EDM. Results in Table 1 show that a smaller minimum thickness can be obtained without the water flushing.

4. SEM investigation

The SEM is applied to examine the surface, subsurface cross-section, and debris of the wire EDM cut thin-section to gain insight of possible causes that limit the EDM thin-section cutting.

4.1. Nd–Fe–B thin-section

Fig. 6 shows SEM micrographs of three Nd–Fe–B magnet thin-sections shown in Fig. 3. These three thin-sections were machined by wire EDM with respective T_{on} settings of 18, 10, and 6 μs. The roughness of the surface was measured using a Taylor Hobson Form Taylorsurf contact profilometer. The measured values of arithmetic surface roughness R_a, also shown in Fig. 6, are 3.40, 1.16, and 0.90 μm for $T_{on}=18$, 10, and 6 μs, respectively. Rougher surface with larger crater and deeper subsurface damage can be identified on the EDM Nd–Fe–B thin-section. Below the thin surface recast layer, there does not seem to be much difference on the three Nd–Fe–B samples. This observation of the shallow subsurface damage is a step toward the hypothesis for limited thickness of cross-section in wire EDM cutting.

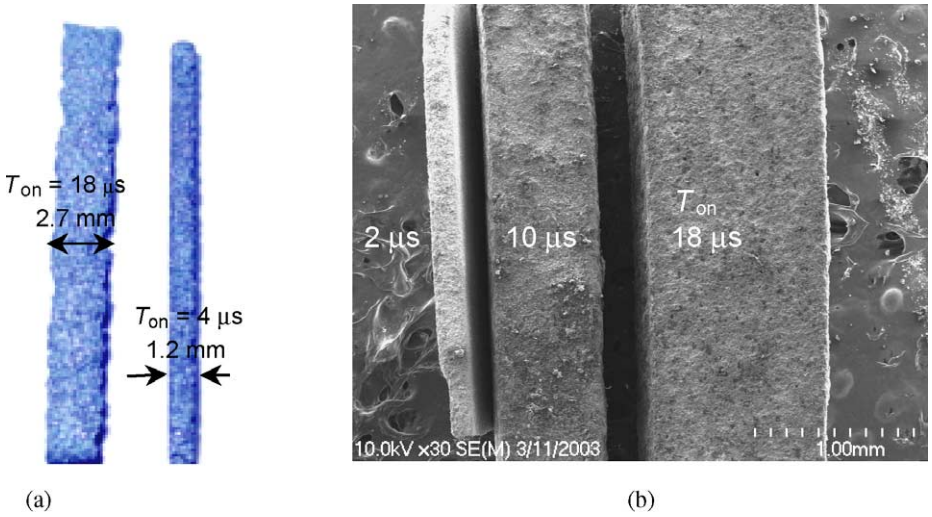

Fig. 5. Minimum thickness by wire EDM thin-section of: (a) carbon–carbon bipolar plate and (b) Nd–Fe–B magnet.

Table 1
EDM thin section cutting of sintered Nd–Fe–B magnet

With water flushing			Without water flushing		
T_{on} (μs)	T (μs)	Minimum thickness (mm)	T_{on} (μs)	T (μs)	Minimum thickness (mm)
2	80	0.20	2	80	0.15
10	120	0.75	6	80	0.35
18	150	1.15	10	80	0.53
			14	120	0.67
			18	200	0.95

4.2. Nd–Fe–B debris

A trap made of filter paper is set up in the wire EDM machine to capture the EDM debris during machining. Debris in two tests, one during regular EDM cutting and another during the failed thin-section EDM cutting, are captured and examined using the SEM. The failed thin-section EDM cutting means the setup for EDM cutting a section with thickness slightly smaller than the known minimum thickness. The intent is to observe the EDM debris to gain insight on wire EDM of thin cross-section.

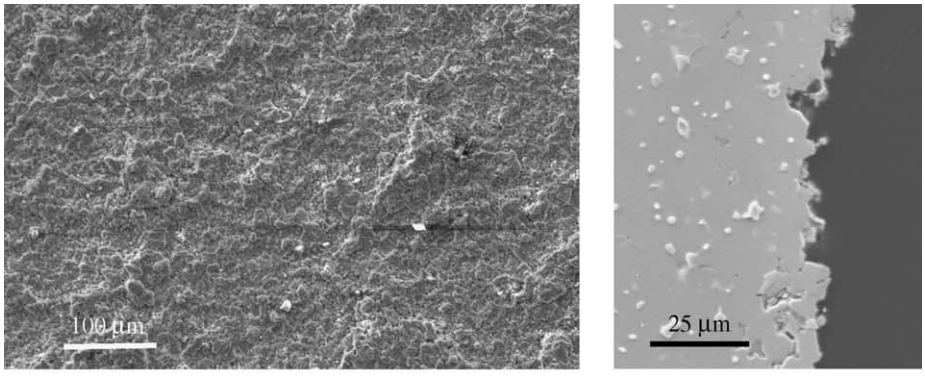

(a) T_{on} = 18 μs, R_a = 3.40 μm

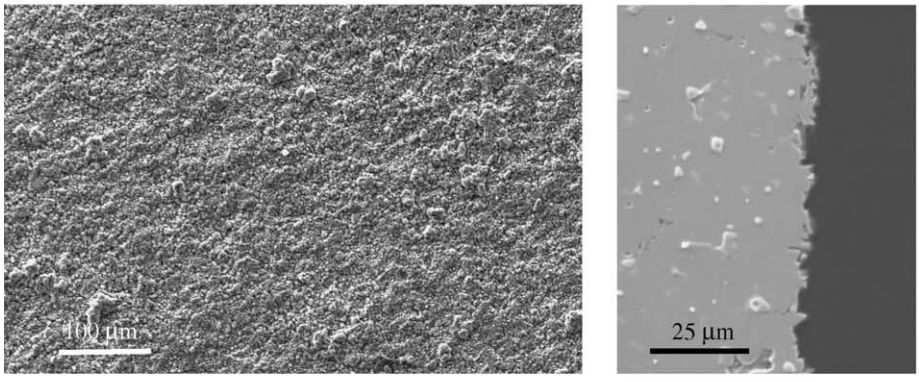

(b) T_{on} = 10 μs, R_a = 1.16 μm

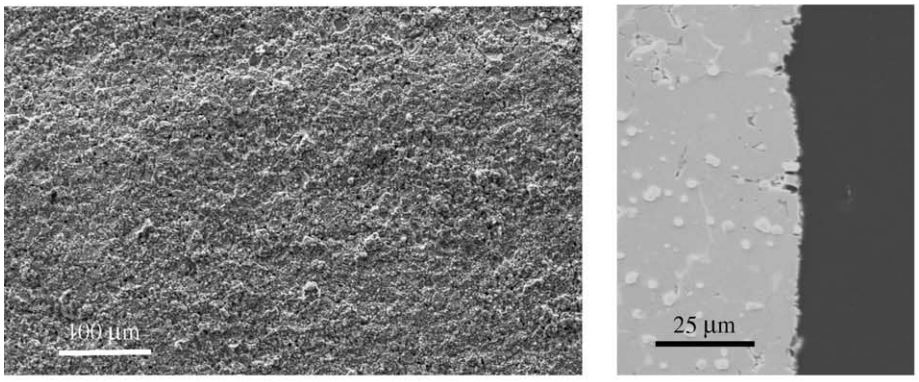

(c) T_{on} = 6 μs, R_a = 0.90 m

Fig. 6. SEM micrographs of surface and cross-section of the subsurface generated on the Nd–Fe–B thin-section machined by wire EDM.

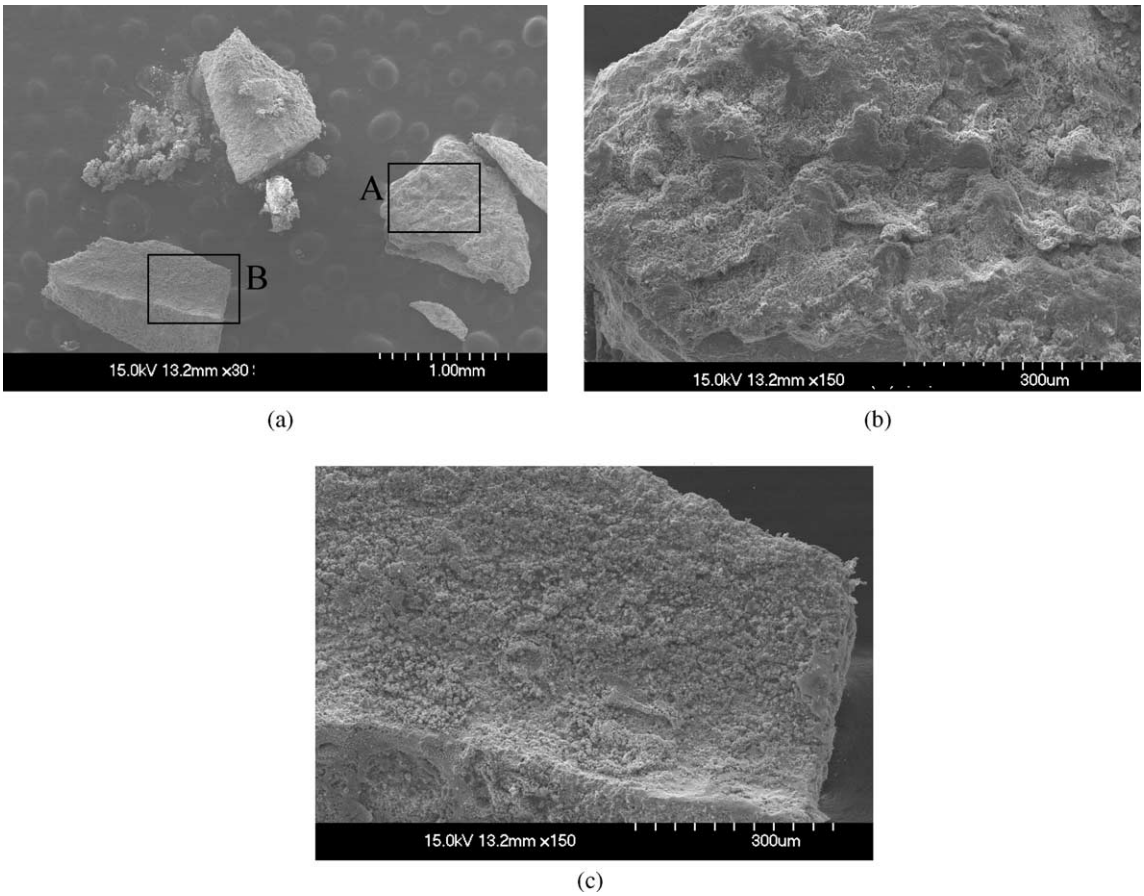

Fig. 7. SEM micrographs of debris from regular wire EDM of Nd–Fe–B with $T_{on}=6$ μs: (a) overview of debris, (b) close-up view of box A in (a), and (c) close-up view of box B in (a).

Figs. 7 and 8 show the debris captured in regular and failed thin-section EDM cutting, respectively. Both tests have $T_{on}=6$ μs and $T=80$ μs. In the regular EDM cutting, relatively large chuck of debris with the size close to 0.8 mm was observed. It is noted that only the large particles were captured during the test. Smaller particles have been either flushed away or captured inside the filter media. The size of captured particles is much larger than the traditional molten and resolidified EDM debris and indicated the brittle fracture due to thermal stress occurred during the EDM process. In the close-up view of a debris particle in Fig. 7(b), the EDM recast layer, similar to that of Fig. 6, is observed. On the other cross-section view of debris in Fig. 7(c), the cleave fractured surface can be seen. This indicates that the particle was disengaged from the workpiece by fracture. Nd–Fe–B is a very brittle material with the fracture

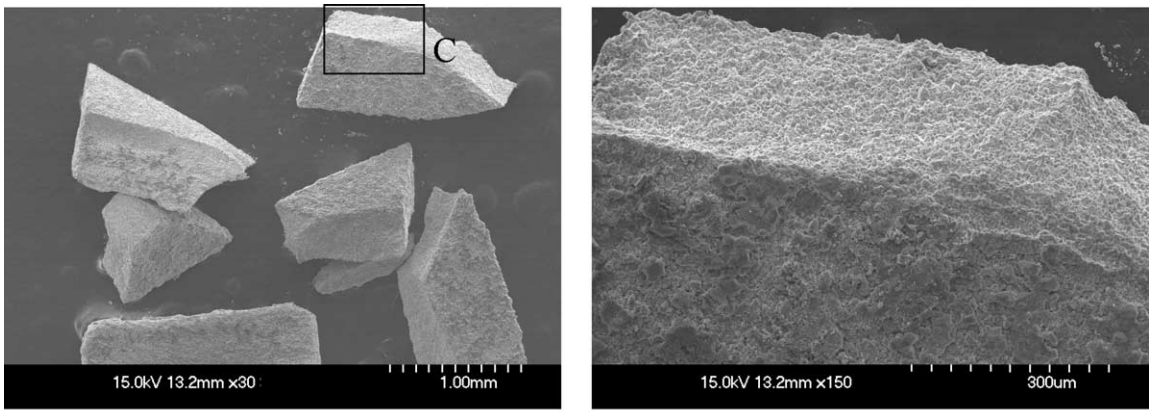

Fig. 8. SEM micrographs of debris in failed thin-section wire EDM cutting with $T_{on}=6$ μs: (a) overview of debris and (b) close-up view of the box C in (a).

toughness K_{IC} only in the 2.5–5.5 MPa $m^{1/2}$ [17]. Its resistance to tensile stress produced by thermal shock is not good. The same phenomenon of thermal cracking the Nd–Fe–B material can also be identified in Fig. 8 for the debris particle of failed thin-section cutting. Large, about 0.9 mm size, debris with clear cleave surface is observed.

The Nd–Fe–B debris collected in regular EDM and failed thin-section EDM with $T_{on} = 10$ μs and $T = 80$ μs are also examined using the SEM. The same conclusion, as demonstrated in Figs. 7 and 8, is reached.

5. Hypothesis of fracture in EDM thin-section cutting

The observations in Figs. 6–8 indicate that the stress fracture, particularly the tensile stress for the brittle Nd–Fe–B, limits the thickness in thin-section wire EDM cutting. Two possible sources of stress that causes the fracture are the thermal stress and electrostatic stress.

EDM is a thermal process and thermal stress is generated around the crater after the spark erosion. Yadav et al. [18] has applied the finite element method to analyze the thermal stress induced by a single spark in EDM of Cr die steel. The high temperature gradient is observed in a small heat affected zone as deep as 0.1 mm. The thermal stress was large and dominated by tensile stresses. Such high thermal stress can cause the fracture in thin-section cutting of the brittle Nd–Fe–B work-material.

This study extended the finite element analysis of thermal stress to the specific thin-section EDM cutting configuration. The coupled temperature and stress analysis using ANSYS finite element analysis software is conducted. The finite element mesh used in this analysis is shown in Fig. 9(a). The 2D 4-node plane stress finite element is selected. For the coupled analysis, each node has three degree-of-freedom: the temperature and displacements in X and Y directions. The Nd–Fe–B workpiece is 2.15 mm high and 1.16 mm wide. The width of the groove and the diameter of the semi-circle at the end of groove is 0.3 mm. The depth of the groove is 1.15 mm. Width of the thin-section is 0.06 mm. The entire surrounding region is under force convection cooling except the semi-circular front region of the groove, which is assumed to be 1620 K, melting temperature of sintered Nd–Fe–B, for a period of 18 μs, the duration of T_{on}. After the first 18 μs of heating, the semi-circular region, like all the other surrounding regions, is cooled by convective heat transfer in the next 62 μs to make the 80 μs spark cycle. Another spark duration of 18 μs and 1620 K on the semi-circular region of the groove is applied and then followed by the 62 μs cooling. The same 18 μs heating and 62 μs cooling procedure repeats for the third time. The transient, coupled thermal and stress analysis was performed. In the stress analysis, the bottom right corner node is fixed in the X and Y directions and the bottom left node is fixed only in the Y direction. Material properties used for the input are: 7500 kg/m^3 density, 160 GPa Young's modulus, 0.24 Poison's ratio, 420 J/kg K heat capacity, 9 W/m K thermal conductivity, 3 μm/m K thermal expansion coefficient, and 2000 W/m^2 K forced convection coefficient.

The temperature and stress distributions at the end of three spark cycles (240 μs after the start of the first spark) are illustrated in Fig. 9(b) and (c). A thin layer of high temperature at about 980 K is concentrated in front of the semi-circular groove region. High tensile thermal stress at about 250 MPa, which is the same value as the flexural strength of Nd–Fe–B, is located close to the semi-circular groove region where the periodical melting temperature applied. The EDM subsurface has cracks and other

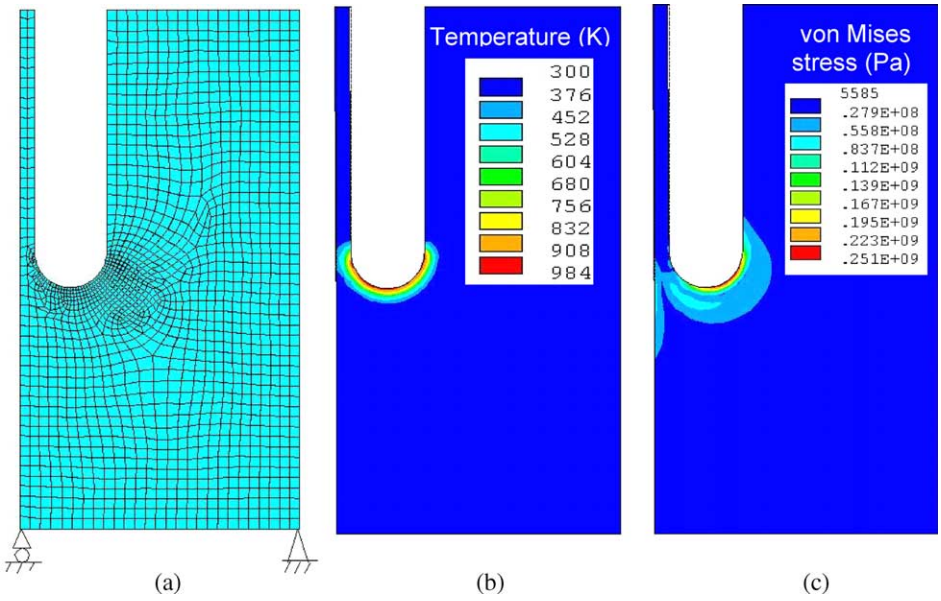

Fig. 9. Finite element prediction of the temperature and thermal stress in thin-section cutting: (a) finite element mesh and boundary condition and (b) contour of temperature, and (c) contour of von Mises stress.

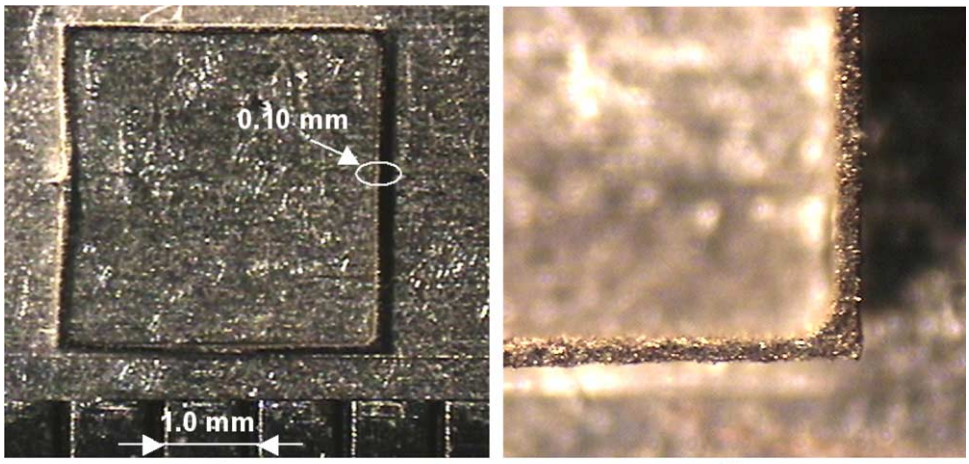

Fig. 10. A 0.1 mm thick 3 mm×3 mm Ti square machined using wire EDM: (a) overview and (b) close-up view of the 0.101 mm thick section.

damages, the flexural strength is expected to much lower than the 250 MPa level. At the location close to the thin-section, the thermal stress is very low, less than 28 MPa. It is likely that only thermal stress alone is not adequate to fracture the thin-section.

Another possible cause of the material removal in EDM, as presented by Singh and Ghosh [19], is the electrostatic force. For very short spark on-time ($T_{on}<5$ μs), the work-material does not have enough time to get the adequate heat for melting. The electrostatic force acting on the surface becomes an important factor for material removal.

It is likely the combination of both thermal and electrostatic stress dominate the cross-section thickness. A further study is underway to model the combined stress to fracture the thin-section in EDM cutting.

6. Application for Ti compliant mechanism manufacturing

The knowledge gained from wire EDM thin-section cutting is applied to manufacture compliant mechanisms. Two examples, both using 1 mm thick Ti plate as the blank, are presented. Fig. 10(a) shows a 3.5 mm×3.5 mm Ti square with 0.1 mm section thickness cut by the wire EDM. The close-up view of one of four corners and the 0.101 mm cross-section thickness, measured using an optical microscope, is shown in Fig. 10(b).

Another example is a Ti compliant mechanism used for variable-focus reflector. This compliant mechanism, as shown in Fig. 11, is about 11 mm×9 mm in size. Fig. 11(a) explains the function of the variable-focus reflector. With the top anchor fixed, the input port in the bottom can be controlled by a piezoelectric actuator to change the curvature and focal length of the top curved region. The thickness of the in-plane cross-section ranges from 0.10 to 0.20 mm, whereas the out-of-plane thickness is 1 mm. The process parameters for fabrication of miniature compliant mechanisms are obtained from the envelope of MRR of Ti (Fig. 3). Two sets of EDM process parameters, corresponding to the high MRR ($T_{on}=18$ μs and $T=80$ μs) and another to the low MRR ($T_{on}=2$ μs and $T=60$ μs), are investigated. The low MRR setting was the process parameter used to

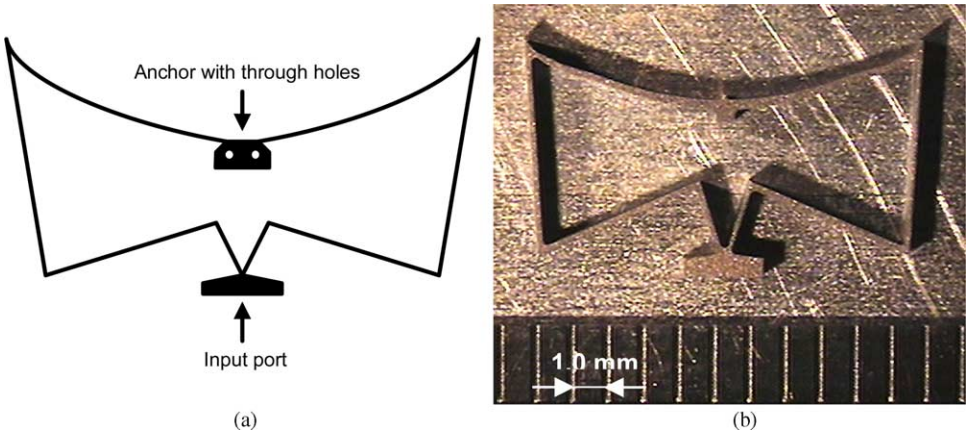

Fig. 11. The variable-focus reflector compliant mechanism: (a) description and (b) wire EDM mechanism with about 0.1 mm in thickness ($T_{on}=2$ μs).

produce the compliant mechanism shown in Fig. 11(b). The fabrication was not successful with the high MRR for the 0.1 mm section thickness.

7. Concluding remarks

Effects of spark cycle and pulse on-time on wire EDM micro features were investigated. Tests were conducted on various materials for minimum thickness wire EDM cutting. Applications of low MRR EDM cutting for machining of thin-section and compliant mechanisms were studied. A hypothesis was proposed based on the combined thermal and electrostatic force to cause the fracture of thin-section during wire EDM. This was supported by findings from SEM micrographs of EDM surface, subsurface, and debris. Further in-depth research is required to understand the root-cause for the material fracture mechanism.

This study presented the needs of detailed thermal and electrostatic stress modeling for micro EDM, particularly for components with miniature feature size. Although results presented are machine-dependent, this research provides the guidelines and procedures for the development of wire EDM process to manufacture miniature features on advanced engineering materials.

Acknowledgements

The authors acknowledge Magnequench and Dr B.M. Ma for the sintered Nd–Fe–B permanent magnets, Porvair PLC, Dr K. Butcher for the metal foam and carbon–carbon bipolar plate, Dr S. Kota on the design specification of compliant mechanisms, Enhui Shi for machine operation, and Rui Li for finite element analysis. A portion of this research was sponsored by the Assistant Secretary for Energy Efficiency and Renewable Energy, Office of Transportation Technologies, as part of the High Temperature Materials Laboratory User Program, Oak Ridge National Laboratory, managed by UT-Battelle, LLC for the U.S. Department of Energy under contract number DE-AC05-00OR22725.

References

[1] S.F. Miller, A.J. Shih, J. Qu, Investigation of the spark cycle on material removal rate in wire electrical discharge machining of advanced materials, International Journal of Machine Tools and Manufacture 44 (2004) 391–400.
[2] J. Qu, A.J. Shih, R.O. Scattergood, Development of the cylindrical wire electrical discharge machining process: part II: surface integrity and roundness, Journal of Manufacturing Science and Engineering 124 (4) (2002) 708–714.
[3] T. Masuzawa, H.K. Tonshoff, Three-dimensional micromachining by machine tools, Annals of the CIRP 46 (1997) 621–628.
[4] Z.Y. Yu, T. Masuzawa, M. Fujino, Micro-EDM for three-dimensional cavities-development of uniform wear method, Annals of the CIRP 47 (1998) 169–172.
[5] T. Masuzawa, K. Okajima, T. Taguchi, M. Fujino, EDM-lathe for micromachining, Annals of the CIRP 51 (1) (2002) 355–358.
[6] Y.F. Luo, An investigation into the actual EDM off-time in SEA machining, Journal of Materials Processing Technology 74 (1998) 61–68.
[7] K. Takahata, Y.B. Gianchandani, Batch mode micro-electro-discharge machining, Journal of Microelectromechanical Systems 11 (2) (2002) 102–110.
[8] K. Furutani, T. Enami, N. Mohri, Three-dimensional shaping by dot-matrix electrical discharge machining, Precision Engineering 21 (1997) 65–71.
[9] K. Furutani, T. Enami, N. Mohri, Dot-matrix electrical discharge machining for shaping fine structure, Proceedings of the IEEE Micro Electro Mechanical Systems (MEMS) 1997; 180–185.
[10] K.P. Rajurkar, Z.Y. Yu, 3D micro-EDM using CAD/CAM, Annals of the CIRP 49 (2000) 127–130.
[11] K. Hori, Y. Murata, Wire electrical discharge machining of micro-involute gears, Transactions of the Japan Society of Mechanical Engineers, Part C 60 (1994) 3957–3962.
[12] Z.Y. Yu, J. Kozak, K.P. Rajurkar, Modeling and simulation of micro EDM process, Annals of the CIRP 52 (2003) 143–146.
[13] P.C. Kaminski, M.N. Capuano, Micro hole machining by conventional penetration electrical discharge machine, International Journal of Machine Tools and Manufacture 43 (2003) 1143–1149.
[14] W. Zhao, Z. Wang, S. Di, G. Chi, H. Wei, Ultrasonic and electrical discharge machining to deep and small hole on titanium alloy, Journal of Materials Processing Technology 120 (2002) 101–106.
[15] S.F. Miller, A.J. Shih, Investigation the effect of spark cycle on the material removal rate in wire electrical discharge machining. 2003 ASME IMECE, Washington, DC, November 16–21, 2003.
[16] L.L. Howell, Compliant Mechanisms, Wiley, London, 2002.
[17] J.A. Horton, J.W. Herchenroder, Fracture toughness of commercial magnets, IEEE Transactions on Magnets 32 (1996) 4374–4376.
[18] V. Yadav, V.K. Jain, P.M. Dixit, Thermal stresses due to electrical discharge machining, International Journal of Machine Tools and Manufacture 42 (2002) 877–888.
[19] A. Singh, A. Ghosh, A thermo-electric model of material removal during electric discharge machining, International Journal of Machine Tools and Manufacture 39 (1999) 669–682.